J|A|C|S
ARTICLES

Published on Web 05/18/2009

Open-Cage Fullerene-like Graphitic Carbons as Catalysts for Oxidative Dehydrogenation of Isobutane

Chengdu Liang,[†,*] Hong Xie,[†] Viviane Schwartz,[†,*] Jane Howe,[‡] Sheng Dai,[†,§] and Steven H. Overbury[†,§]

Center for Nanophase Materials Sciences, Materials Science and Technology Division, and Chemical Sciences Division, Oak Ridge National Laboratory, Oak Ridge Tennessee, 37831

Received February 4, 2009; E-mail: liangcn@ornl.gov; schwartzv@ornl.gov

Abstract: We report herein a facile synthesis of fullerene-like cages, which can be opened and closed through simple thermal treatments. A glassy carbon with enclosed fullerene-like cages of 2−3 nm was synthesized through a soft-template approach that created open mesopores of 7 nm. The open mesopores provided access to the fullerene-like cages, which were opened and closed through heat treatments in air and inert gas at various temperatures. Catalytic measurements showed that the open cages displayed strikingly higher activity for the oxidative dehydrogenation of isobutane in comparison to the closed ones. We anticipate that this synthesis approach could unravel an avenue for pursuing fundamental understanding of the unique catalytic properties of graphitic carbon nanostructures.

1. Introduction

Oxidative dehydrogenation (ODH) of alkanes to alkenes has assumed great relevance in the polymer industry for an energy-efficient conversion of hydrocarbons to polymers. Carbon was identified as an active catalyst for the ODH reaction when acid catalysts were tested for ODH of ethylbenzene. In this case, coke deposited on the catalyst was actually the active layer.[1] A number of publications on carbon catalysts for ODH were published in the past few years. Activated carbons,[1−3] carbon nanotubes,[4] carbon nanofibers,[5] onionlike carbon, and nanodiamonds[4,6] have been closely examined by different groups. However, identifying the catalytic sites of carbon catalysts is a long-standing challenge due to the complexity of the carbon matrix and the lack of spectroscopic measurements. Undetermined mineral impurities, oxygenated functionalities, dangling bonds, and mixed sp^2 and sp^3 hybridization carbon atoms could all contribute to the catalytic activity of carbons in ODH reactions. Typically, the catalytic performance of carbon catalysts has been evaluated as an ensemble of many kinds of potentially active sites. In this sense, a tight control and simplification of the structure of carbon would be of great importance for elucidation of the catalytic behavior of carbons in ODH reactions. Graphitic carbons with controlled open edges and functionalities could be suitable models for the investigation of active sites in carbon catalysts. However, because of the low population of edge sites and functionalities on graphite, their low catalytic activity hinders the precise measurement of the products through traditional detection methods such as gas chromatography. Thus, high-surface-area nanostructured graphitic carbons are promising candidates for the exploration of the catalytic sites of carbon catalysts in ODH reactions.

Since the discovery of carbon nanotubes (CNTs) and fullerenes, the graphitic cavities inside these nanostructured carbons have attracted much attention because of the novel properties emerging from their unique electronic properties,[7] spatial confinement,[7] and atomic smoothness.[8,9] These novel properties have stimulated interest in the exploration of synthetic methods to open and close these cavities in a controlled manner. The nonhexagonal carbon rings at the ends of CNTs are less resistive to oxidation than the hexagonal carbon rings along the tube wall of CNTs; therefore, the ends of CNTs can be selectively opened through various oxidation approaches. Similar oxidative approaches have less success in opening the fullerene cages. Although the "molecular surgery" can open and close the endohedral fullerene cages, the tedious multistep synthesis procedure and laborious separation of the products hamper its applicability for researchers who require large amounts (grams) of material. Two discoveries have made the fullerenes and fullerene-like carbon structures available in very large scale: one is the top-down synthesis of fullerenes through the pyrolysis of polypyrrole nanoparticles;[10] the other is the discovery of fullerene-like structures in commercially available glassy

[†] Center for Nanophase Materials Sciences.
[‡] Materials Science and Technology Division.
[§] Chemical Sciences Division.

(1) Pereira, M. F. R.; Orfao, J. J. M.; Figueiredo, J. L. *Appl. Catal., A* **1999**, *184*, 153–160.
(2) Pereira, M. F. R.; Orfao, J. J. M.; Figueiredo, J. L. *Appl. Catal., A* **2000**, *196*, 43–54.
(3) Pereira, M. F. R.; Orfao, J. J. M.; Figueiredo, J. L. *Appl. Catal., A* **2001**, *218*, 307–318.
(4) Zhang, J.; Su, D. S.; Zhang, A. H.; Wang, D.; Schlogl, R.; Hebert, C. *Angew. Chem., Int. Ed.* **2007**, *46*, 7319–7323.
(5) Zhao, T. J.; Sun, W. Z.; Gu, X. Y.; Ronning, M.; Chen, D.; Dai, Y. C.; Yuan, W. K.; Holmen, A. *Appl. Catal., A* **2007**, *323*, 135–146.
(6) Su, D. S.; Maksimova, N. I.; Mestl, G.; Kuznetsov, V. L.; Keller, V.; Schlogl, R.; Keller, N. *Carbon* **2007**, *45*, 2145–2151.
(7) Pan, X. L.; Fan, Z. L.; Chen, W.; Ding, Y. J.; Luo, H. Y.; Bao, X. H. *Nat. Mater.* **2007**, *6*, 507–511.
(8) Holt, J. K.; Park, H. G.; Wang, Y. M.; Stadermann, M.; Artyukhin, A. B.; Grigoropoulos, C. P.; Noy, A.; Bakajin, O. *Science* **2006**, *312*, 1034–1037.
(9) Majumder, M.; Chopra, N.; Andrews, R.; Hinds, B. J. *Nature* **2005**, *438*, 44–44.
(10) Jang, J.; Oh, J. H. *Adv. Mater.* **2004**, *16*, 1650–1653.

carbons.[11,12] Nevertheless, the utilization of the fullerene-like cavities is complicated by the difficulty of opening the cavities in a controlled manner. Thermal oxidation was used successfully to open the cavities at the outer layer of micrometer-sized glassy carbons.[13] Graphitic cavities with a broad distribution of opening diameters resulted from the oxidation of fullerene-like structures. Cavities at the outermost surface of the glassy carbon particles were widely opened and subjected to the destruction of the graphitic structure due to deep oxidation, while the cavities underneath the oxidized surface film remained intact and closed. Such a heterogeneous structure results from the limited diffusion of oxygen during the oxidation process; namely, the superficial layer of the glassy carbon particles is subjected to longer oxidation time than the core of the particle because of the lack of access of the oxygen to the core. We and others demonstrated that the "soft-template synthesis" is a versatile approach for the synthesis of uniform mesoporous carbon materials with controlled pore sizes and periodicity.[14−18] The mesoporosity of the carbon can be preserved even after treatment at extremely high temperature of more than 2600 °C at which the amorphous carbon has been converted to glassy carbon that has a graphitic structure.[19,20] Since the pore walls of mesoporous carbon synthesized by the soft-template method are only a few nanometers thick, this fact inspired us to speculate about the structure of the glassy carbon that bears uniform mesopores. Does the mesoporous glassy carbon have the closed fullerene-like cavities that are found in the commercial glassy carbons? If so, can the cavities be uniformly opened through oxidation utilizing the mesopores to provide a full access of oxygen to the interior of carbon particles? Can the openness and the chemical functionalities of the fullerene-like cavities be controlled through physical and chemical modifications? Is there any new property arising from controlled openness of the fullerene-like cavities?

In this work, we explore the fullerene-like cavities of the mesoporous glassy carbon through heating treatments and oxidation. The openness and oxygen content of the fullerene-like cavities were varied systematically through deliberate synthesis conditions. The resulting model carbons were structurally characterized and tested for their activity and selectivity in an ODH reaction. The results give insights to the active sites of carbon catalysts and reveal that the open cavities of the fullerene-like structures are the most active sites for the selective ODH of isobutane to isobutene.

2. Experimental Section

2.1. Synthesis. 2.1.1. Chemicals. Pluronic surfactant F127 (Sigma-Aldrich), phloroglucinol (99.9% Sigma-Aldrich), hydrochloric acid 37 wt % (Sigma-Aldrich), formaldehyde 37 wt % aqueous solution (Sigma-Aldrich), and 200 proof ethanol (Pharmco Aaper) were used as received. Air was supplied by a compressed air cylinder purchased from Air Product, and 2% O_2 (balance N_2) and 4% i-C_4H_{10} (balance N_2) were purchased from Air Liquid.

2.1.2. Procedure. The aperiodic mesoporous carbon was prepared by using a modified procedure reported by Liang and Dai.[16] In a typical preparation, F127 (12.6 g), phloroglucinol (25.2 g), and hydrochloric acid 37 wt % aqueous solution (5 g) were dissolved in 650 mL of absolute ethanol. The solution was then refluxed with vigorous stirring at 80 °C for 15 min. An aqueous solution of formaldehyde 37 wt % was added to the reaction mixture in two steps separated by a 1 h interval. First, 5 g of the solution was added while 8 g of the solution was added in the second step, followed by continued stirring for another hour. Orange particles were collected from the reactants through filtration, washed twice with 10 mL of ethanol each, and then dried overnight at 80 °C. This polymeric material was then pyrolyzed in N_2 in a tube furnace (Thermolyne, model 79300) by ramping the temperature to 850 °C at 2 °C/min. The final temperature was kept for 2 h to ensure the completion of carbonization. The resultant carbon materials were then transferred to a graphite furnace (Thermal Technologies, model 1000-2560-FP20), in which they were treated at 2600 °C in helium for 1 h through a ramp of 40 °C/min. The sample heat-treated at 2600 °C was denoted as SC01. Starting with SC01, a set of carbon samples with variable functionalities and opened/closed edges was prepared using a sequence of treatment procedures. The sample identified as SC02 was prepared by oxidation of SC01 in air at 500 °C for 15 h; SC02 was further heat-treated in helium for 1 h at 1600 °C and denoted as SC03; SC04 was obtained by heat treatment of SC03 to 2600 °C in helium.

2.2. Structural Characterization. 2.2.1. High-Resolution Transmission Electron Microscopy (HR-TEM). HR-TEM images were taken on HF-3300 field emission TEM that operated at 300 kv. TEM samples were prepared by grinding the carbon samples with an agate mortar and pestle. The particles were first dispersed in acetone and then loaded to a TEM grid. The solvents were removed in a vacuum oven at 80 °C overnight.

2.2.2. Nitrogen Sorption. Nitrogen adsorption isotherms of the porous carbons were measured at 77 K by using a Micromeritic Gemini 275 system. The specific surface areas and pore size distributions were calculated by using the Brunauer−Emmett−Teller (BET) theory and the Barrett−Joyner−Halenda method based on the adsorption branches of the isotherms. The specific pore volumes were measured at relative pressure 0.95.

2.2.3. Thermogravimetric Analysis (TGA). TGA was conducted on a TA Q-500 TGA system (TA Instruments). Platinum pans were preheated to 1000 °C in air for 2 h and cooled to room temperature before the samples were loaded. The TGA measurement was run under an air flow of 50 SCCM. The temperature was stepped to 500 °C within 2 min and then kept for 1400 min.

2.2.4. Powder X-ray Diffraction (PXRD). PXRD patterns were recorded at a PANalytical X'pert PRO 2-circle X-ray diffractometer. The samples were ground by a mortar and pestle and loaded on a silicon zero-background sample holder.

2.2.5. Temperature-Programmed Desorption (TPD). The surface-oxygenated functionalities were characterized by TPD. The release of CO and CO_2 at different temperatures was employed as the signals for the assignment of the oxygenated functional groups, although some controversy exists in the literature regarding the proper assignment of the TPD peaks.[21] In this work, the measurements were carried out in a U-tube reactor (Altamira AMI-200) in flowing helium (30 mL/min) with a heating rate of 5 K min^{-1}. The amounts of CO and CO_2 desorbed were measured by a quadrupole mass spectrometer (Pfeiffer-Balzer Omnistar) equipped with a 1-m-

(11) Harris, P. J. F. *Philos. Mag.* **2004**, *84*, 3159–3167.
(12) Harris, P. J. F. *Crit. Rev. Solid State Mater. Sci.* **2005**, *30*, 235–253.
(13) Braun, A.; Bartsch, M.; Schnyder, B.; Kotz, R.; Haas, O.; Wokaun, A. *Carbon* **2002**, *40*, 375–382.
(14) Liang, C.; Li, Z.; Dai, S. *Angew. Chem., Int. Ed.* **2008**, *47*, 3696–3717.
(15) Liang, C. D.; Hong, K. L.; Guiochon, G. A.; Mays, J. W.; Dai, S. *Angew. Chem., Int. Ed.* **2004**, *43*, 5785–5789.
(16) Liang, C. D.; Dai, S. *J. Am. Chem. Soc.* **2006**, *128*, 5316–5317.
(17) Meng, Y.; Gu, D.; Zhang, F. Q.; Shi, Y. F.; Yang, H. F.; Li, Z.; Yu, C. Z.; Tu, B.; Zhao, D. Y. *Angew. Chem., Int. Ed.* **2005**, *44*, 7053–7059.
(18) Zhang, F. Q.; Meng, Y.; Gu, D.; Yan, Y.; Yu, C. Z.; Tu, B.; Zhao, D. Y. *J. Am. Chem. Soc.* **2005**, *127*, 13508–13509.
(19) Shanahan, P. V.; Xu, L. B.; Liang, C. D.; Waje, M.; Dai, S.; Yan, Y. S. *J. Power Sources* **2008**, *185*, 423–427.
(20) Wang, X. Q.; Liang, C. D.; Dai, S. *Langmuir* **2008**, *24*, 7500–7505.
(21) Figueiredo, J. L.; Pereira, M. F. R.; Freitas, M. M. A.; Orfao, J. J. M. *Carbon* **1999**, *37*, 1379–1389.

long gas sampling capillary followed by an apertured entrance into the turbo-pumped quadrupole chamber.

2.3. Catalytic Test. Catalytic experiments were conducted in a commercial laboratory-scale, fixed-bed reactor (PID − Microactivity Reactor System). An amount of 0.2 g of catalyst was used in each run and was placed in a vertically positioned stainless steel tubular reactor under atmospheric pressure at 400 °C. The feed composition for the reaction was 4% i-C_4H_{10} and 2% O_2, and balance N_2. The gas flows were monitored by a mass controller system calibrated for each gas. The total flow rate of the feed was fixed for all ODH runs at 40 sccm, which is equivalent to a gas hourly space velocity of 5100 h^{-1}. The effluents were sampled through transfer valves and analyzed using an Agilent 6890 gas chromatographer (GC) equipped with a Hayesep N column and a molecular sieve column connected to a flame ionization detector (FID). CO and CO_2 were converted to CH_4 through a methanizer before they passed though the FID detector for analyses. Under these reaction conditions, the main products (above 99%) detected from the reaction were i-C_4H_8, CO, and CO_2. The absence of homogeneous gas-phase contribution was verified by using quartz beads on the place of the carbon catalysts. These blank runs showed no activity at 400 °C. Calculation of the mass balance was based on a carbon balance and was confirmed within ±5% by quantitative analysis of reactants and products. The conversion of isobutane, the isobutene selectivity, and the activity were calculated using the following equations:

$$X = \frac{F_{i\text{-}C_4H_{10},\text{in}} - F_{i\text{-}C_4H_{10},\text{out}}}{F_{i\text{-}C_4H_{10},\text{in}}} \times 100\% \quad (1)$$

$$S = \frac{F_{i\text{-}C_4H_8,\text{out}}}{F_{i\text{-}C_4H_{10},\text{in}} - F_{C_4H_{10},\text{out}}} \times 100\% \quad (2)$$

$$a = \frac{F_{i\text{-}C_4H_{10},\text{in}} \times X}{W} \quad (3)$$

where X is the conversion of isobutane, S is the selectivity of isobutene, a is the activity based on the reaction rate of isobutane, W is the weight of the catalyst, and F is the flow rate.

3. Results and Discussion

3.1. Structural Evolution of Carbon Catalysts. Except for a few exceptions, the pyrolysis of cross-linked polymers usually results in hard carbons, which are also known as nongraphitizing carbons.[22] High-temperature treatment up to 3000 °C causes nongraphitizing carbon to evolve into closed nanocages of fullerene-like structures.[11,23] Recently, we found that the mesoporosity developed through the soft-template method can survive high-temperature treatment as high as 2600 °C.[20] The resulting mesoporous carbon possesses a graphitic structure and strongly resists catalytic oxidation when used as catalyst support for fuel-cell cathode.[19] The inertness of the high-temperature-treated carbons most likely originates from their continuous graphitic structures. In this research, we intend to open the fullerene-like structure through a controlled air oxidation at a temperature that allows the oxidation of defects and amorphous carbon while preserving the graphitic part of the fullerene-like cavities. According to previous research, the C_{60} and the ends of CNTs can be slowly oxidized at 500 °C while the graphitic part of the CNT remains intact.[24] Therefore, the temperature for air oxidation was carefully selected as 500 °C and monitored by TGA. Shown in Figure 1 is the TGA of isothermal treatment of the graphitized mesoporous carbon (GMC) in air at 500 °C. The GMC slowly loses weight by oxidative gasification of carbon. The gasification rate (dW/dt) increased along with the heating time and displayed a typical sigmoidal curve that sped up at the beginning and change of gasification rate slowed after the inflectional point at about 700 min. The maximum gasification rate of carbon reached 0.065% per minute when the GMC was heated in air for 24 h. Such a slow reaction rate ensures that the oxidation of the GMC is a reactivity-controlled rather than a diffusion-controlled process. Therefore, GMC can be homogeneously oxidized by air. SC02 was synthesized by oxidation of SC01 in air for 20 h at 500 °C, resulting in a 35% weight loss.

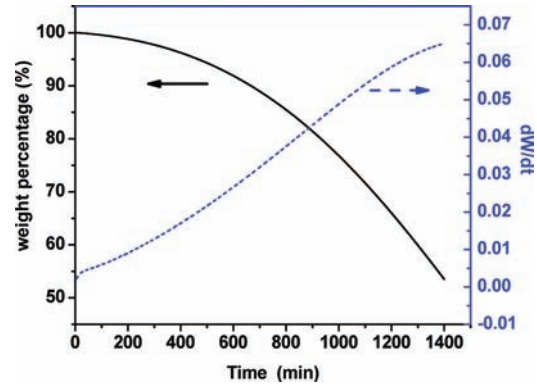

Figure 1. Isothermal TGA curve and the derivative of weight change versus time of SC01 heated at 500 °C with an air flow of 50 sccm.

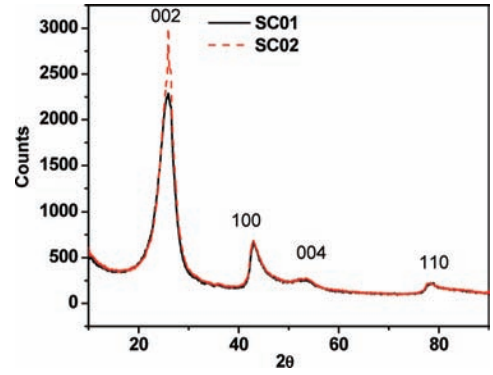

Figure 2. Powder X-ray diffraction patterns of graphitized mesoporous carbons before (SC01) and after (SC02) oxidation.

The integrity of the graphitic structure of SC02 was verified by PXRD. Shown in Figure 2 is a comparison of the PXRD patterns of GMC before (SC01) and after (SC02) oxidation. The PXRD patterns possess similar features with four distinguishable peaks at 2θ equal to 26.1°, 43.0°, 53.6°, and 78.2° that are indexed as graphite (002), (100), (004), and (110) peaks, respectively. It is worth noting that the (002) peak became slightly sharper after the oxidation. The plausible explanation is that the carbons with less graphitic structure, most likely the defect sites,[25] the small crystallites, and the non-six-member rings on the curved fullerene-like structures, were burnt off during air oxidation. After 35% weight loss corresponding to losses of the small crystallites and defect sites, the relatively

(22) Franklin, R. E. *Proc. R. Soc. London, Ser. A* **1951**, *209*, 196–218.
(23) Harris, P. J. F.; Tsang, S. C. *Philos. Mag. A* **1997**, *76*, 667–677.
(24) (a) Ajayan, P. M.; Ebbesen, T. W.; Ichihashi, T.; Iijima, S.; Tanigaki, K.; Hiura, H. *Nature* **1993**, *362*, 522–525. (b) Tsang, S. C.; Harris, P. J. F.; Green, M. L. H. *Nature* **1993**, *362*, 520–522.
(25) Lee, S. M.; Lee, Y. H.; Hwang, Y. G.; Hahn, J. R.; Kang, H. *Phys. Rev. Lett.* **1999**, *82*, 217–220.

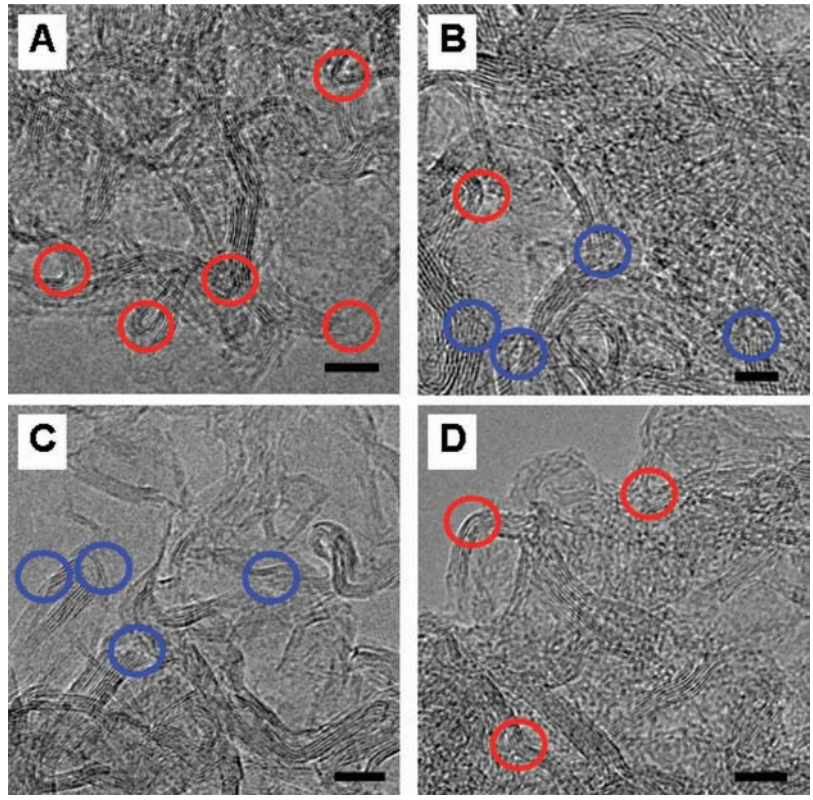

Figure 3. HR-TEM images of samples (A) SC01, (B) SC02, (C) SC03, and (D) SC04. Red circles indicate the "loop back structures", whereas blue circles indicate the open edge sites of the graphitic carbon. Scale bars represent 5 nm.

larger crystallites were retained and gave a slightly sharper signal on the (002) peak. Therefore, the air oxidation of SC01 to SC02 with less than 35% weight loss was not detrimental to the graphitic structure of GMC.

The graphitic structures of the carbon samples were further confirmed by the HR-TEM images. The fringes of the graphite crystallites were distinctly presented on all HR-TEM images shown in Figure 3 that were taken throughout the sequence of samples from SC01 to SC04. The fullerene-like cavities were observed in all samples. This fact confirmed that the GMC has the same structure of commercial glassy carbons except for its mesoporosity created by the soft-template approach. Figure 3A shows the structure of SC01, the pristine GMC. The image presents enclosed fullerene-like cavities with the size of 2−3 nm that coincide with the literature values.[11,23] Indicated by the red circles in Figure 3A,B are the sharp turns of the graphitic structures. These turns are most likely the defects of the graphitic structures or a small amount of the amorphous carbon. Similar structures were observed in the thermal coalescence of CNTs at temperatures higher than 1600 °C.[26−28] These sharp turns are also referred to as the "loop-back" structure.[29] The "loop-back" does not have the perfect six-member ring structure. Therefore, these sites are more reactive than the basal plane of graphitic carbon. The oxidation of the GMC led to the gasification of carbon atoms at these "loop-back" sites. Consequently, the fullerene-like carbon cavities were opened through the oxidation. The air oxidation resulted in three changes to the GMC. First, the internal surface of the fullerene-like cavities with diameters around 2−3 nm was exposed. These open cavities were further confirmed by nitrogen absorption measurements that are described later in this section. Second, oxygenated functional groups were attached to the carbon surface. The oxygenated functionalities were assigned by TPD experiments discussed in section 3.2. Third, the oxidation created open edges on graphite. The open edges were clearly present in sample SC02, and open edges also were preserved in the SC03 that was prepared by heating SC02 to 1600 °C in helium. The blue circles in Figure 3B,C indicate the open edge sites of the graphitic carbon. SC04 was a product of further heating of the SC03 sample to 2600 °C in helium. Its microstructure in Figure 3D is akin to that of SC01, the pristine GMC, as shown in Figure 3A. Therefore, the heat treatment of SC03 to 2600 °C closed both the open edges and the fullerene-like cavities as well.

To further confirm the structural changes of the GMC, we monitored the changes of the surface areas, pore volumes, and pore size distributions along with the heating treatments by BET measurements (Figure 4 and Table 1). These four samples have type IV isotherms with H1 hysteresis. The lower closure points of all samples are at relative pressure (P/P_0) 0.35. The hysteresis loops in samples SC01 and SC04 are slightly wider than those of samples SC02 and SC03. The changes of the hysteresis loops in the sequence of the four samples suggested the following conclusions: (1) the pristine GMC (SC01) has relatively narrow interconnection among the mesopores, (2) the air oxidation widens the interconnections of mesopores, therefore leading to a narrowed hysteresis loop in SC02, (3) the heating treatment

(26) Metenier, K.; Bonnamy, S.; Beguin, F.; Journet, C.; Bernier, P.; de La Chapelle, M. L.; Chauvet, O.; Lefrant, S. *Carbon* **2002**, *40*, 1765–1773.
(27) Kim, U. J.; Gutierrez, H. R.; Kim, J. P.; Eklund, P. C. *J. Phys. Chem. B* **2005**, *109*, 23358–23365.
(28) Gutierrez, H. R.; Kim, U. J.; Kim, J. P.; Eklund, P. C. *Nano Lett.* **2005**, *5*, 2195–2201.
(29) Endo, M.; Lee, B. J.; Kim, Y. A.; Kim, Y. J.; Muramatsu, H.; Yanagisawa, T.; Hayashi, T.; Terrones, M.; Dresselhaus, M. S. *New J. Phys.* **2003**, *5*, 121.

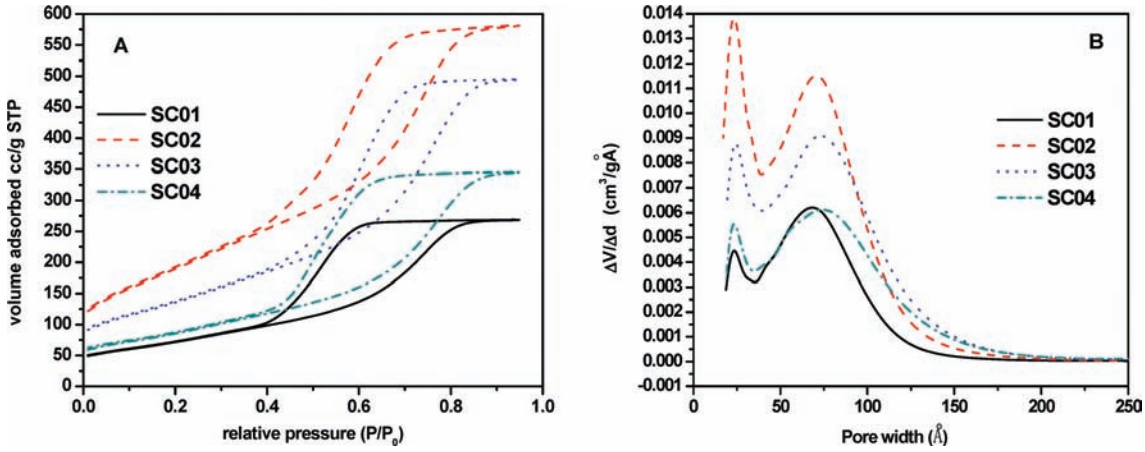

Figure 4. (A) Nitrogen absorption/desorption isotherms measured at 77 K. (B) Calculated pore size distribution.

Table 1. Specific Surface Area and Pore Volume of GMC after Heating Treatments

sample	SC01	SC02	SC03	SC04
specific surface area (m^2/g)	265	693	497	316
specific pore volume (cm^3/g)	0.416	0.898	0.766	0.534

in helium to 1600 °C (SC03 sample) has no obvious influence on the interconnection of the mesopores, and (4) the heat treatment of SC03 to 2600 °C narrows the pore interconnections, therefore leading to a wider hysteresis loop in the isotherm of sample SC04.

The pore size distributions of the four samples are bimodal, each exhibiting maxima near 2.5 and 7 nm. The small mesopores have a narrow distribution between 2 and 3 nm, while the large mesopores are broadly distributed between 4 and 13 nm. The oxidation and heat treatments did not alter the position of the maximum of the 2.5-nm pores. However, there is a slight shift of the maximum for the large mesopores from 6.8 nm for SC01 to 7.5 nm for SC04. Therefore, the oxidation and heat treatments on the carbon samples slightly influenced the size of the large mesopores but not the small mesopores. The large and small pores are of different origins; the large mesopores resulted from the decomposition of "soft templates",[16] and the small mesopores resulted from fullerene-like cavities that are created by the graphitization process.[11,12,23] Therefore, the slight enlargement of the mesopores can be attributed to the oxidation of the fullerene walls. The specific surface area and pore volume of the pristine GMC increased after the oxidation. The pore volume of the GMC increased from 0.416 cm^3/g (SC01) to 0.898 cm^3/g after oxidation (SC02). The increased pore volume is mainly attributed to the voids in the fullerene-like cavities caused by the oxidative pitting at the defect sites as observed by HR-TEM. Evidently, the fullerene-like cavities in SC01, the pristine GMC, are not fully accessible by N_2 in the BET measurements because of their closed structure; the air oxidation opened the cavities and made them measurable by BET. The BET measurements also validated the results of the HR-TEM characterization and confirmed that the GMC has a similar fullerene-like structure that is ubiquitous in commercial glassy carbons. The pore volume and surface area of the oxidized GMC (SC02) slightly decreased when it was heated to 1600 °C (SC03), and those parameters of SC03 significantly decreased after it was reheated to 2600 °C (SC04). The specific surface area and pore volume of SC04 is comparable to those of SC01 after the air oxidation and followed by reheating to 2600 °C. Similar reversibility was observed when comparing the microstructures of SC01 and SC04 shown in Figure 3A,D. The fullerene-like cavities in SC01 and SC04 are mainly closed and contrasting from the open cavities in SC02 and SC03. Therefore, the opening and closing of the fullerene-like cavities are evidently reversible, although a complete reversibility was not attained in the sequence of sample preparation. The minor difference of surface area and pore volume between SC01 and SC04 is most likely caused by a destructive step during the oxidation, which is not completely recoverable in the subsequent reheating step.

3.2. TPD Analysis of Oxygenated Surface Functionalities. As mentioned above, the air oxidation could result in oxygenated functionalities on the surface of the carbon. These functionalities were characterized by TPD measurements. The oxygenated species on the carbon surface thermally decompose to CO and CO_2 during the heating of carbon samples in helium. Because each functional group decomposes at different temperature, the evolution of CO and CO_2 as a function of temperature can be used to assign the functional groups empirically.[21] Figure 5A,B shows the evolution of CO and CO_2 during TPD on the four carbon samples. The CO signals in SC01, SC03, and SC04 were negligible, and only weak CO_2 signals were detected in these three samples that are most likely from the physical absorbed CO_2 in the samples. Contrasting from the other three samples, SC02 gave strong signals of CO and CO_2 desorption at various temperature. The CO peak at 700 °C of SC02 in Figure 5A could be assigned as the ether group with oxygen as a heteroatom in the six-member ring.[21] The shoulder peak at 900 °C in the CO analysis could relate to the decomposition of carbonyl and/or quinone groups. Very high CO_2 peaks were also observed at temperatures below 800 °C, which could be assigned to the carbonyl and quinone as well.[21] The TPD assignments of oxygenated functionalities could be very rough because of the lack of appropriate spectroscopic analysis for functional groups on the black carbon surface. Nevertheless, the striking high volume evolution of CO and CO_2 of SC02 strongly suggests that the surface of SC02 was oxygenated, while the other three samples have very low levels of oxygen. Because the only oxygen source in the TPD experiments is the adsorbed oxygen on the carbon surface, either chemically absorbed as oxygenated groups or physically absorbed oxygen, CO, and CO_2, the total oxygen calculated from the TPD results based on the CO and CO_2 can be used as an indicator of the

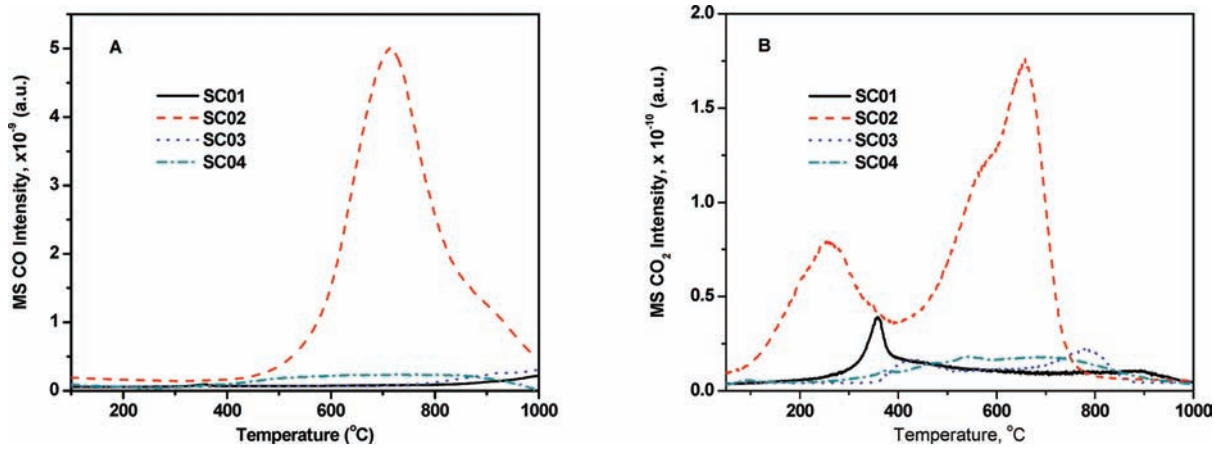

Figure 5. TPD analysis of carbon samples in helium. (A) CO and (B) CO_2 evolution.

Table 2. CO and CO_2 Desorption from Oxygen-Containing Groups of Carbons by TPD

sample	SC01	SC02	SC03	SC04
CO (μmol/g)	N/D	1875	N/D	50
CO_2 (μmol/g)	13	82	10	10
total oxygen atom (μmol/g)	26	2039	20	70

total oxygen absorption capacity of the carbon catalysts. Summarized in Table 2 are the amounts of CO, CO_2, and the converted total oxygen concentration that were measured by TPD. The total oxygen concentration of SC02 is about 2.2 atom % and is two magnitudes higher than that of SC01 and SC03. Evidently, the surface of SC02 is functionalized through oxygenated species. The total oxygen concentration on SC04 is slightly higher than that on SC01, indicating that the destructive oxidation of the fullerene-like carbon cages is not fully reversible.

Summarizing, distinct structural properties were observed for the four carbons. SC01 is the pristine GMC with close fullerene-like cavities; SC02 has both open fullerene-like cavities and oxygenated functionalities; SC03 has open fullerene-like cavities but without oxygenated functionalities; and SC04 has returned to a closed, oxygen-free structure nearly like SC01. The relationship between the microstructures and functionalities of these four samples and their catalytic performances will be discussed in the following section.

3.3. ODH of *i*-C_4H_{10} Reaction for Carbon Catalytic Test. All four samples were tested as catalysts for the ODH reaction. Catalytic activities of carbon catalysts were calculated on the basis of the reaction rate of isobutane by using eq 3. The selectivity was calculated using eq 2. Data plotted in Figure 6 were the reaction rates (solid symbols) and selectivities (open symbols) shown as a function of time-on-stream (TOS). Both SC01 and SC04 showed low activity in the ODH reactions. The reaction for SC01 in the first 6 h was below the GC detection limit. Very low activity (less than 0.3% *i*-C_4H_{10} conversion) was observed after 6 h with a high selectivity about 80% toward *i*-C_4H_8. SC04 had a very low initial activity (0.4% *i*-C_4H_{10} conversion) that was increased by a factor of 2 after 20 h of TOS. The overall reactivity of SC04 was an order of magnitude lower than those of SC02 and SC03. The selectivity of SC04 was about 50% toward *i*-C_4H_8. In contrast, SC02 and SC03 were highly active for the ODH reaction with an average selectivity of 62% toward *i*-C_4H_8 at steady state. Interestingly, SC03 was slightly more active than SC02 in the first 12 h with a steady

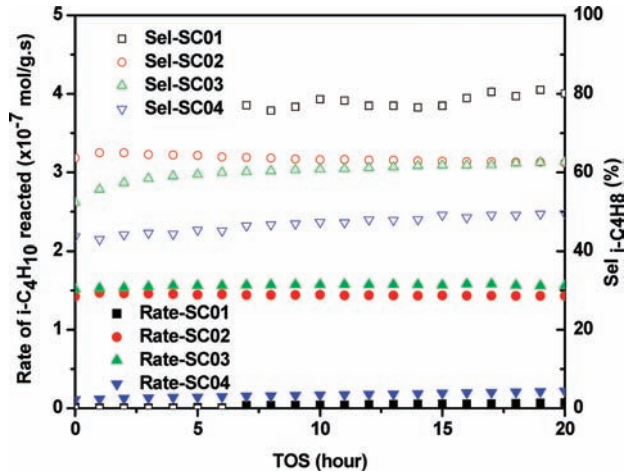

Figure 6. Evolution of the ODH of *i*-C_4H_{10} to *i*-C_4H_8 in terms of catalytic activity and selectivity with TOS of 20 h.

increase of activity during the entire 20 h test. Although the selectivity of SC03 was initially lower than that of SC02, it increased with TOS and had the same selectivity as SC02 by the end of the 20 h test. Nevertheless, the difference in activity for these two catalysts was negligible. Both catalysts are highly active and stable in the ODH reactions. Considering the structural differences of these carbon samples, we could conclude that the catalytic activities of GMC in ODH reaction are related to the open cavities of the fullerene-like structure. Since SC02 and SC03 contain very different amounts of oxygen but are so similar in catalytic performance, we conclude that the presence of oxygenated functionalities does not crucially affect either the activity or the selectivity of the catalyst. Although SC01 showed the highest selectivity in the four catalysts, the controlling cause of the selectivity is still unknown. Further investigation is necessary for the elucidation of selectivity. Generally speaking, graphitic carbon contains two planes: the edge plane and the basal plane. The edge plane is usually more reactive than the basal plane. The graphitic structures in glassy carbon are curved and form continuous fullerene-like structures with loops; therefore, the basal plane dominates the surface of glassy carbon.[11,12] Such a continuous structure is quite inert in reactions; thus, SC01 and SC04 were essentially inactive in the ODH reactions. The curving apexes of the fullerene-like structures are the defects of the graphitic structure. They are less stable than the basal plane and could be oxidized by air and pitted through at 500 °C. Consequently, the edge

plane was exposed at the orifice of the pits. SC02 and SC03 had the open edge planes resulting from the air oxidation. Therefore, these open edge planes could be the active center for the ODH reaction. The difference between SC02 and SC03 is that the open edge planes in SC02 were covered by oxygenated functional groups, while in SC03, these oxygenated groups were stripped away through thermal treatment in helium at 1600 °C. Since the reaction was conducted in low conversion conditions, the remaining oxygen in the reaction stream could possibly oxidize the dangling bonds at the open edge planes in SC03 to form surface oxygen-containing groups. Therefore, we cannot rule out the possible contributions of the catalytic activity from the oxygenated groups. Nonetheless, the open edge plane is a prerequisite for the activity of glassy carbon in the ODH reactions.

4. Conclusions

We demonstrated that high-temperature treatments on mesoporous amorphous carbon can convert it to a GMC with structure typical of glassy carbon, although the graphitic pore walls are only a few nanometers thick. Closed fullerene-like cavities were observed in this GMC. These cavities can be uniformly opened through air oxidation at 500 °C without affecting the graphitic structure of the glassy carbon. A secondary porosity of 2.5-nm size with complementary oxygenated functionalities was made accessible after oxidation. The oxygenated functionalities can be thermally removed by heating the carbon materials in helium at 1600 °C without affecting the openness of the cavities. Reheating of the oxidized GMC to 2600 °C caused the open fullerene-like cavities to close. Therefore, the fullerene-like cavities can be opened and closed reversibly through air oxidation and heat treatment.

The GMCs showed obvious catalytic activities in the ODH reactions when the fullerene-like cavities were open, regardless of the existence of the surface-oxygenated functionalities. The GMC catalysts were deactivated after the fullerene-like cavities were closed by thermal treatment. Therefore, the catalytic activity is related to the openness of the fullerene-like cavities. The open cavities have accessible graphitic planes with open edges. These open edges were most likely the active sites of the carbon catalysts in the ODH reactions.

Acknowledgment. This research was supported by the Center for Nanophase Materials Sciences, which is sponsored at Oak Ridge National Laboratory by the Scientific User Facilities Division, Office of Basic Energy Sciences, U.S. Department of Energy.

JA900888P